# New Isotopes of Thorium Studied with an Improved Helium-Jet Recoil Transport Apparatus*

KALEVI VALLI AND EARL K. HYDE
*Lawrence Radiation Laboratory, University of California, Berkeley, California 94720*
(Received 14 June 1968)

Five neutron-deficient isotopes of thorium lighter than mass 218 were studied at the Berkeley Heavy Ion Linear Accelerator by bombardment of enriched $^{206}$Pb with $^{16}$O. Silicon (Au) surface-barrier detectors were used in on-line measurements performed to determine $\alpha$-decay characteristics. Mass-number assignments of $^{213}$Th through $^{217}$Th were made on the basis of excitation functions and systematic trends in $\alpha$-decay properties. Half-lives and $\alpha$-particle energies were determined. New information was also obtained about the $\alpha$-decay characteristics of $^{216}$Ac, $^{215}$Ra, $^{214}$Fr, and $^{212}$At. Systematic occurrence of complex structure in the $\alpha$ decay of even-$Z$ 125-neutron nuclei is discussed, and spins and parities are suggested for three lowest-energy levels of $^{211}$Ra, $^{209}$Rn, and $^{207}$Po. Systematic occurrence of isomerism in odd-$Z$ 127-neutron nuclei is also discussed, and spins and parities are suggested for several levels. On the basis of the extreme regularity of the experimental $\alpha$ energies, predictions are made for the energies of several unknown neutron-deficient isotopes of thorium, protactinium, uranium, and neptunium. In the experimental work, the helium-jet transport method was used to remove the $\alpha$-emitting products from the target region. Technical details concerning the application of the method to millisecond activities are discussed.

## I. INTRODUCTION

THIS paper deals chiefly with the discovery of five thorium isotopes with mass numbers ranging from 213 to 217 produced at the Berkeley Heavy Ion Linear Accelerator (HILAC) by bombardment of $^{206}$Pb targets with beams of $^{16}$O and studied by on-line techniques of $\alpha$ spectroscopy. For nuclei with $Z=90$ these are extremely deficient in neutrons but the extra stability associated with the 126-neutron shell decreases the $\alpha$-decay energies enough so that half-lives are lengthened to the range of milliseconds to seconds. This study represents an extension of our previous studies of the $\alpha$-decay properties of isotopes lying near or below the 126 neutron shell of the following elements: polonium and astatine,[1] radon,[2] francium,[3] radium,[4] and actinium.[5] This series of studies together with previously available information[6] makes it possible with considerable accuracy to interrelate many nuclei in the group of nuclides with more than 82 protons and 127 or fewer neutrons and to derive important properties such as atomic masses, neutron and proton binding energies, etc.

In the present work it was necessary to make some modification in the experimental techniques to permit faster collection of the recoil nuclei. As a result of this greater collection speed it was possible to obtain new information on several isotopes containing 127 neutrons, which were unobserved or incompletely studied in the papers published previously. In Sec. III C there is a discussion of results on $^{214}$Fr, $^{215}$Ra, $^{216}$Ac, and $^{217}$Th.

Compound nucleus reactions involving as their first step the complete fusion of the $^{16}$O projectile and $^{206}$Pb target were required for the preparation of the thorium isotopes and the characteristics of these reactions (principally the shape of the excitation function) were used in the identification of the mass numbers of the new isotopes. In the course of the work considerable information was collected on the excitation curves for lower $Z$ products (principally isotopes of radium and francium) which prove that reactions of incomplete fusion play a prominent role in their formation. In Sec. IV the new results are correlated with previous data and the present state of the systematics of $\alpha$ decay for this region of the system of nuclides is reviewed. In Sec. IV we also discuss the energy levels revealed in the complex $\alpha$ decay of odd mass nuclei with 125 neutrons and the occurrence of isomerism in odd-odd nuclei with 127 neutrons. Some detailed comments on the experimental techniques including suggestions for their extension to study of $\gamma$ radiations emitted by the collected recoil atoms are presented in the Appendix.

## II. EXPERIMENTAL

### A. Helium Jet Transport System

The experimental technique is based on the work of Ghiorso[7] and of Macfarlane and Griffioen.[8,9] In its essentials, the method consists of the slowing down of the product nuclei recoiling out of a thin target by collisions with helium gas atoms in a small target chamber filled with helium. The helium streams out of this chamber through a small orifice into an adjacent vacuum chamber and carries with it the radioactive

* This work was performed under the auspices of the U. S. Atomic Energy Commission.

[1] W. Treytl and K. Valli, Nucl. Phys. **A97**, 405 (1967).
[2] K. Valli, M. J. Nurmia, and E. K. Hyde, Phys. Rev. **159**, 1013 (1967).
[3] K. Valli, E. K. Hyde, and W. Treytl, J. Inorg. Nucl. Chem. **29**, 2503 (1967).
[4] K. Valli, W. Treytl, and E. K. Hyde, Phys. Rev. **161**, 1284 (1967).
[5] K. Valli, W. J. Treytl, and E. K. Hyde, Phys. Rev. **167**, 1094 (1968).
[6] E. K. Hyde, I. Perlman, and G. T. Seaborg, *The Nuclear Properties of the Heavy Elements* (Prentice-Hall, Inc., Englewood Cliffs, N. J., 1964), Vol. II, pp. 991–1107.
[7] A. Ghiorso (unpublished).
[8] R. D. Macfarlane and R. D. Griffioen, Nucl. Instr. Methods **24**, 461 (1963).
[9] R. D. Macfarlane, in *Proceedings of the International Conference on the Physics of Heavy Ions, Dubna, 1966* (Joint Institute for Nuclear Studies, Dubna).

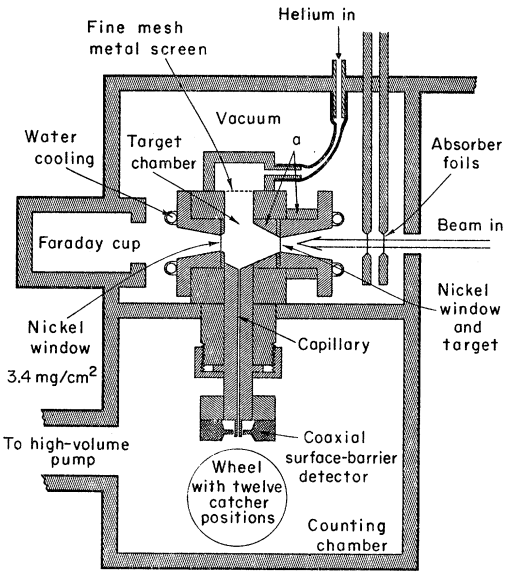


FIG. 1. Schematic diagram of the present apparatus.

recoil products. This gas jet impinges on a metallic surface upon which the recoil nuclei are collected. The $\alpha$ decay of the collected nuclei can be detected by a semiconductor detector facing the collector or, alternatively, the collector can be transported by some mechanical device to the detector.

The apparatus which we employed in our previous research[1,5] proved to be inappropriate for the present study because the time between product formation and detection was too long. Our present system is illustrated in Fig. 1. In the interest of rapid collection the target chamber was made small. The minimum distance from the target entrance window to the nickel exit window was 12 mm but it could be lengthened by insertion of two extension tubes marked *a* in Fig. 1. In most experiments the chamber length was 20 mm but a few half-life measurements were performed with the minimum size chamber. On the suggestion of Ghiorso, helium was introduced at the top of the chamber through a double thickness of electromesh grid to reduce turbulence and to direct the gas flow smoothly toward the bottom of the chamber. The helium stream out of the chamber passed through a 0.41-mm-diam capillary 5.5 cm long. The tip of this capillary in the lower vacuum chamber passed through a central hole in a silicon (gold) surface barrier detector with an active area of 50 mm². The detector was manufactured by Ortec Inc., Oak Ridge, Tennessee. The gas stream emerged from the tip of the capillary and impinged on a stainless-steel surface located 5–8 mm from the front surface of the detector. The collector consisted of a 12-position wheel whose drive mechanism could be activated electrically to turn a clean surface or an $\alpha$ calibration standard before the detector. We are indebted to R. D. Macfarlane for the idea of the capillary and the detector with the central hole. The water cooling coils on the window assemblies reduced window failures and prevented a drift in the output of the semiconductor detector caused by a steady rise in the temperature of the whole apparatus during bombardments.

The helium pressure was varied at the beginning of each set of experiments to determine the value giving the highest yield of the thorium isotopes. Most data reported in this paper were taken at an absolute pressure of 1.9 atm. The helium flow rate was 60 cm³/sec. From this and the cross section of the capillary (0.13 mm²) the velocity of the helium at exit was 460 m/sec and the kinetic energy of an atom of mass 216 swept along with it was 0.24 eV.

In the system illustrated in Fig. 1, the time between production and detection is determined by only two factors: (1) how long it takes to slow down and sweep the recoil nucleus out of the chamber in the gas jet and (2) how soon after the beam burst the detector can be gated on. When the target chamber was operated at the minimum size, the volume was about 1.0 cm³. To remove this amount of gas through the capillary required 17 msec. However, some fraction of the activity was collected in a much shorter time. This 17 msec turnover time meant that nuclides with half-lives much shorter than 17 msec underwent considerable decay before collection and the observed intensities of these peaks do not reflect the true production rates for these nuclides. It also meant that in any half-life determination performed during the interval ($\sim$20 msec) between two subsequent beam bursts, both collection and decay of the activity had to be considered.

The long capillary made it possible to shield the detector from the highly radioactive target area. The counter could be gated on immediately after the beam burst and, in fact, it could be used even during the beam bursts although the $\alpha$ spectra taken during the beam-on period had much greater background caused by neutrons and $\gamma$ rays.

Some aspects in the design of the apparatus are discussed in Appendix B.

### B. Bombardment Techniques

The reactions used to produce the thorium activities were

$$^{206}\mathrm{Pb}(^{16}\mathrm{O},xn)^{222-x}\mathrm{Th},$$

where $x$ refers to the number of evaporated neutrons. The target consisted of 2.8 mg/cm² of separated $^{206}$Pb electroplated on 1.7 mg/cm² Cu foil. The $^{206}$Pb was obtained from Oak Ridge National Laboratory and had the following isotopic composition: 97.22% $^{206}$Pb, 1.34% $^{207}$Pb, and 1.39% $^{208}$Pb.

The 166 MeV $^{16}$O beam of the HILAC was bent 15° in a steering magnet and directed through 20 ft of beam pipe before entering the target chamber (Fig. 1) through the entry window consisting of the $^{206}$Pb target, its copper foil backing and a 1.7 mg/cm² nickel foil, the lead deposit being on the inside surface of the

window. The beam energy was varied by inserting stacks of 1.72 mg/cm$^2$ aluminum foils in front of the target. The range-energy relationships of Northcliffe[10,11] were used to calculate the beam energy degradation in the absorber and in the chamber window.

In a typical set of experiments a steady beam current of about 350 nA $^{16}$O was passed through the chamber and measured in a Faraday cup. The run was terminated when the integrated beam reached some selected value. This usually took about 30 min. The products of the reaction were continuously collected and the amplitudes of the $\alpha$ pulses from the detector-amplifier system were measured with a 1024-channel ADC unit interfaced to a PDP-7 computer. The output of the amplifier was gated off during the 5-msec beam bursts. At the end of the run the number of absorbers was changed and a new run began, starting about 10 min after the end of the preceding run. Ten such runs were made until the beam energy was reduced to the Coulomb barrier value which is about 75 MeV. The spectra from all runs were plotted and the areas under individual $\alpha$ peaks computed and replotted as excitation functions (yield-versus-beam-energy curves).

The energy scales for the $\alpha$ spectra were determined in two steps. Primary alpha standards from the actinium and thorium series, in particular $^{211}$Bi 6.6222 MeV, $^{219}$Rn 6.8176 MeV, $^{215}$Po 7.3841 MeV, and $^{212}$Po 8.7854 MeV,[12] were used to determine the energies of prominent peaks assigned in this study to $^{216}$Th, $^{215}$Ra, and $^{214}$Fr. The reaction products and the primary standards were measured simultaneously to eliminate any possibility of shifts due to unknown factors. Then the peaks for those three reaction products plus $^{215}$Ac, 7.605 MeV[5] and $^{214}$Ra, 7.136 MeV[4] were used as internal secondary standards to calibrate the scale for the other peaks in the spectra.

### C. Half-Life Determinations

The measurement of decay periods was done with a special electronic programmer which synchronized the operation of the beam with the recording of spectra during selected time periods and controlled the storage of these spectra in separate parts of the computer memory. The programmer could operate in several modes. In the case of relatively long half-lives such as the 1.2 sec of $^{215}$Th or the 125 msec of $^{214}$Th, analysis was first blocked for a bombardment period of several half-lives to allow the activity to reach a saturation value. Then the beam was turned off by the central programmer and data were collected during 16 equal time periods and stored in 16 sections of the computer memory. Then the beam was turned on again by the programmer and the process was repeated until sufficient statistical accuracy was obtained. A normal overall running time for the half-life determination was 1 or 2 h.

In a faster mode of operation analysis was blocked during the beam bursts and then, during the intervals between subsequent bursts, $\alpha$ pulses were collected in 16 equal time periods and stored in 16 sections of the computer memory. This process was continued for as many beam bursts as necessary to build up sufficient statistical accuracy in the 16 256-channel spectra.

In still another mode of operation analysis was not blocked during the beam. Instead, a timing signal from the accelerator turned on the amplifier output just as the beam pulse started. Then spectra were recorded for 8 or 16 successive time periods spread over the beam pulse and the time between beam pulses. The successive spectra were stored in separate sections of the computer. In this case the spectra from the counting periods covering the beam pulse contained a higher general background. However, many peaks could be resolved and, in particular, important information on certain very short lives peaks, notably $^{217}$Th, could be obtained from an examination of the spectra taken just before and just after the end of the beam pulses.

Owing to the 17-msec turnover time in our chamber the observed count-rate-versus-time curves in the case of the last two modes of operation have a complex shape similar to the growth and decay of a daughter product of radioactive decay. Half-lives determined from the descending parts of these curves are slightly longer than the true half-lives.

## III. RESULTS

### A. General Comments

Figure 2 shows sample spectra taken at representative beam energies. The $\alpha$-emitting products are quite numerous because the nuclear reactions are complex and because many radioactive daughter products are formed in the rapid decay of the primary products.

The compound nucleus is $^{222}$Th and the excitation energies at the Coulomb barrier and at the maximum beam energy are sufficient for the evaporation of 3 and 10 neutrons, respectively. Hence we can expect to form thorium isotopes of mass 219 down to 212 each with a characteristic excitation function. Each of these should reach a maximum at a beam energy most favorable for the evaporation of a certain number of neutrons and decrease at higher beam energies as the probability for the evaporation of one more neutron increases. A series of excitation functions having these characteristics appears in Figs. 3 and 4. From the extreme regularities discussed in our previous papers for the variation of alpha energy versus neutron number near the magic number 126 we can predict with confidence the alpha energies and half-lives of the thorium isotopes. These predictions help us to identify individual isotopes. The predicted and observed half-lives of $^{216}$Th and the lighter isotopes were in a convenient range for our helium

[10] L. C. Northcliffe, Phys. Rev. **120**, 1744 (1960).
[11] L. C. Northcliffe, Ann. Rev. Nucl. Sci. **13**, 67 (1963).
[12] A. Rytz, Helv. Phys. Acta **34**, 240 (1961).

transport system. It was questionable whether our collection time would be fast enough for us to observe $^{217}$Th but we did succeed in identifying it. We expected the half-lives of $^{218}$Th and $^{219}$Th to be too short for detection with our techniques and in fact we did not observe them. We discuss the individual thorium isotopes in Sec. III B.

A second main group of products is the isotopes of

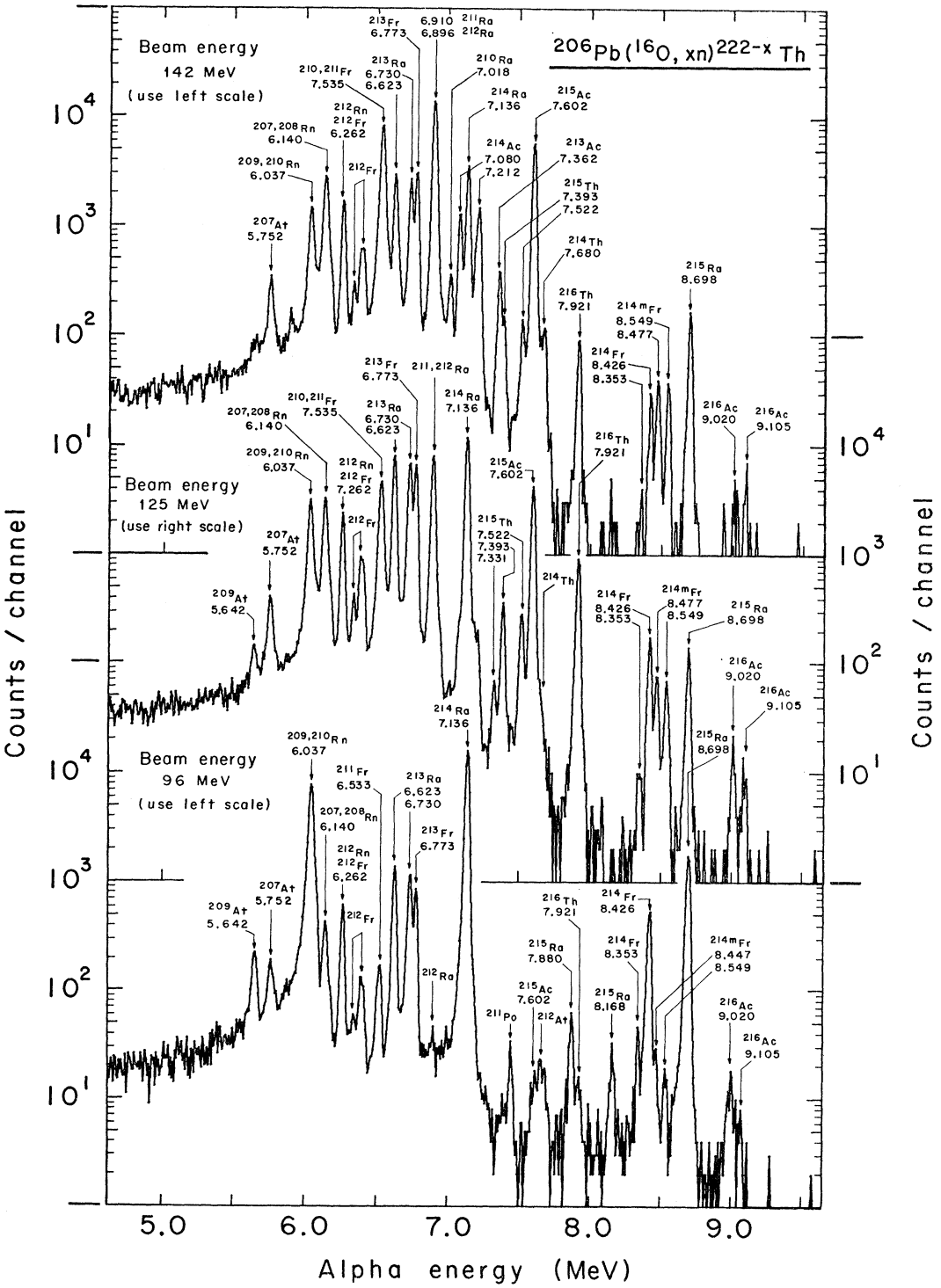


FIG. 2. $\alpha$ spectra showing activities from the $^{206}$Pb+$^{16}$O reactions at three beam energies. The spectra were recorded continuously between beam bursts. The beam current, 0.3 $\mu$A, was integrated over the measuring time, 40 min, to the same total in each measurement. These spectra and others were used to construct the excitation functions shown in Figs. 3 and 4.

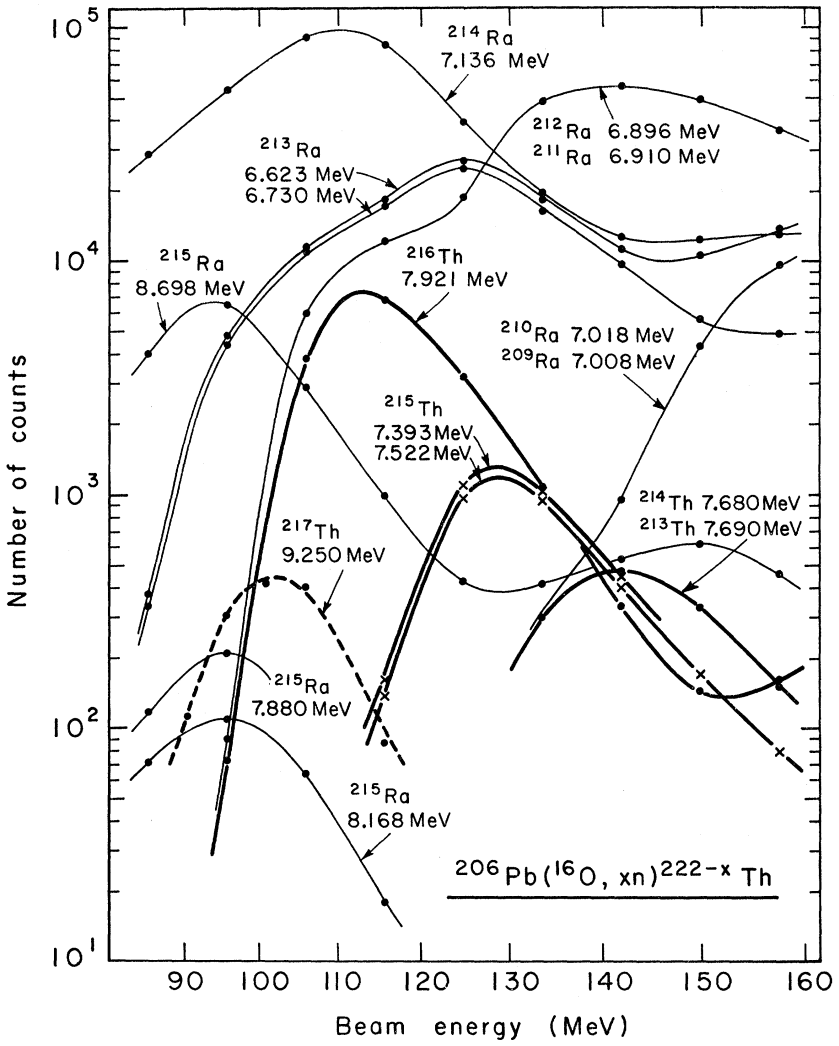


FIG. 3. Excitation functions for the thorium and radium isotopes produced in the $^{206}Pb+^{16}O$ reactions. The experiments were run from high- to low-beam energies with about 10-min intervals between measurements. See the caption of Fig. 2 for other details. The $^{217}Th$ curve was obtained from a separate set of experiments as discussed in Sec. III C *1*.

actinium, radium, francium, radon, astatine, and polonium—particularly those with 126 or fewer neutrons—made by a variety of reactions. Actinium and radium isotopes can be formed by the rapid electron capture or $\alpha$ decay of thorium parent isotopes, But, owing to the large loss of the parent nuclei by nuclear fission, a more likely mode of formation is the direct emission of a proton or an $\alpha$ particle together with several neutrons during the deexcitation of the compound nucleus. The high intensities of the actinium and radium peaks compared to the thorium peaks, as well as the broad excitation functions, are in agreement with this conclusion. One consequence of this is that the presence of actinium and radium isotopes of known mass number is not helpful in the assignments of the thorium mass numbers. Some of the francium, astatine, and polonium activities come from radioactive decay of precursors but a considerable fraction may come from reactions not involving a complete fusion of the target and projectile.

A third category of products is a group of very short-lived nuclides containing 127 neutrons. We obtained some new information on $^{217}Th$, $^{216}Ac$, $^{215}Ra$, and $^{214}Fr$ which we discuss in Sec. III C.

The fact that nuclear fission accounts[13,14] for about three quarters of the total reaction cross section deserves mention for two reasons. First, fission occurs primarily in the excited thorium nuclei formed in the de-excitation of the compound nucleus, so that the yields of thorium isotopes are greatly reduced. The nuclei of lower atomic number do not suffer so much from this fission competition and hence contribute relatively much more to the $\alpha$ spectra. Secondly, the range of the fission products is much larger than that of the $\alpha$-emitting reaction products so that most of the fission products are not stopped in the helium before they strike the walls of the target chamber and hence are not transported out by the helium stream.

[13] H. C. Britt and A. R. Quinton, Phys. Rev. **120**, 1768 (1960).
[14] T. Sikkeland, Phys. Rev. **135**, B669 (1964).

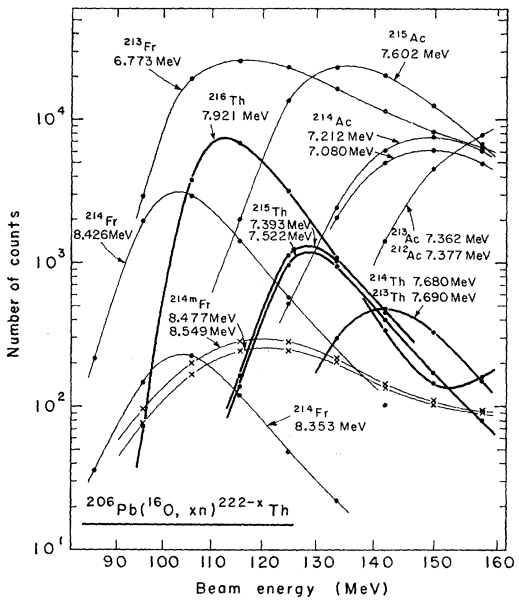


FIG. 4. Excitation functions for the thorium, actinium, and some francium activities produced in the $^{206}Pb+^{16}O$ reactions. See the captions of Figs. 2 and 3 for details.

### B. Thorium Isotopes with 126 or Fewer Neutrons

#### *1. Thorium-216*

From the regularities in $\alpha$-decay properties displayed in Fig. 9 the alpha energy of $^{216}$Th was expected to be between 7.90 and 7.95 MeV and on the basis of the known half-lives of $^{215}$Ac, $^{214}$Ra, $^{213}$Fr, $^{212}$Rn, and $^{211}$At—all nuclei with 126 neutrons—the half-life of $^{216}$Th could be predicted to lie between 10 and 50 msec. In Fig. 2 an $\alpha$ group is presented at 7.921±0.008 MeV. The measured decay period for this group is 28±2 msec. Supporting evidence for the assignment of this activity to $^{216}$Th comes from the excitation function shown in Figs. 3 and 4 which has the shape characteristic of a compound nucleus reaction product. The yield maximum at 114 MeV beam energy corresponds to an excitation energy of 69 MeV for the $^{222}$Th compound nucleus

TABLE I. Excitation energies of the compound nucleus $^{222}$Th at the Coulomb barrier and at the yield maxima of the thorium isotopes. The beam energies corresponding to the maxima were taken from Fig. 3, the masses of $^{16}$O and $^{206}$Pb were obtained from Mattauch *et al.*,[a] and the estimated mass of $^{222}$Th from Viola and Seaborg.[b] The last column gives the average energy release per evaporated neutron in the de-excitation process.

| | $E_{beam}$ (MeV) | $E_{excit.}$ (MeV) | $n$ | $E_{excit./n}$ (MeV) |
|---|---|---|---|---|
| Coulomb barrier | 74.7 | 29.8 | ... | ... |
| $^{217}$Th | 102 | 57 | 5 | 11.4 |
| $^{216}$Th | 114 | 69 | 6 | 11.5 |
| $^{215}$Th | 128 | 83 | 7 | 11.9 |
| $^{214}$Th | 142 | 97 | 8 | 12.1 |
| $^{213}$Th | 157 | 112 | 9 | 12.4 |

[a] Reference 15.
[b] Reference 16.

TABLE II. Summary of thorium results.

| Isotope | $\alpha$ energy (MeV) | Half-life (sec) | % |
|---|---|---|---|
| $^{217}$Th | 9.250±0.010 | <0.0003 | ... |
| $^{216}$Th | 7.921±0.008 | 0.028±0.002 | ... |
| $^{215}$Th | 7.522±0.008 | 1.2±0.2 | 40±3 |
| | 7.393±0.008 | 1.2±0.2 | 52±3 |
| | 7.331±0.010 | 1.2±0.5 | 8±3 |
| $^{214}$Th | 7.680±0.010 | 0.125±0.025 | ... |
| $^{213}$Th | 7.690±0.010 | 0.150±0.025 | ... |

(Table I[15,16]), which is reasonable for the evaporation of six neutrons. Additional support for the assignment comes from the fact that the yield maximum occurs at a beam energy 14 MeV lower than that for the yield maximum of $^{215}$Th which isotope can be identified with certainty on the basis of its distinctive decay properties. It is probable that $^{216}$Th undergoes decay by electron capture to $^{216}$Ac to a slight extent. Our results give an upper limit of 0.6% for such branch decay. The true value could be substantially lower. See Table II.

#### *2. Thorium-215*

From the regularities in properties of other nuclides with 125 neutrons, namely, $^{214}$Ac, $^{213}$Ra, $^{212}$Fr, and $^{211}$Rn, we can expect the $\alpha$ spectrum of $^{215}$Th to have several $\alpha$ groups and thus to be distinguished from neighboring thorium isotopes which are expected to have a single prominent $\alpha$ transition. Furthermore, we can expect the lowest energy group to have an energy between 7.50 and 7.55 MeV. In addition, we can expect $^{215}$Th to have the longest half-life of any thorium isotope prepared in this study.

We assign three groups in our spectra (Fig. 2) to $^{215}$Th: 7.522±0.008 MeV, (40±3)%; 7.393±0.008 MeV, (52±3)%; and 7.331±0.010 MeV, (8±3)%. A half-life of 1.2±0.2 sec was measured for all three groups. The excitation functions of the two most prominent groups are shown in Figs. 3 and 4. The shapes of the curves are typical for a compound nucleus reaction. The maximum yield occurs at a beam energy of 128 MeV, which corresponds to an excitation energy of 83 MeV for the $^{222}$Th compound nucleus. This amount to a reasonable average of 11.9 MeV (Table I) removed in the evaporation of each of the seven neutrons.

The third $^{215}$Th group at 7.331 MeV is most clearly visible at about 125 MeV beam energy because at higher beam energies it is obscured by the intense 7.37 MeV peak that belongs to $^{212}$Ac and $^{213}$Ac.

We looked for a possible electron capture branching of $^{215}$Th by measuring the half-life for $^{215}$Ac observed in bombardments carried out with 125 MeV $^{16}$O ions (i.e., at the peak of the $^{215}$Th excitation function). The

[15] J. H. E. Mattauch, W. Thiele, and A. H. Wapstra, Nucl. Phys. **67**, 1 (1965).
[16] V. E. Viola, Jr., and G. T. Seaborg, J. Inorg. Nucl. Chem. **28**, 297 (1966).

TABLE III. Summary of results on nuclides with 127 neutrons.

| Isotope | This work α energy (MeV) | This work Half-life (msec) | % | Previous report α energy (MeV) | Previous report Half-life (msec) | Ref. |
|---|---|---|---|---|---|---|
| $^{217}$Th | 9.250±0.010 | <0.3 | ... | ... | ... | ... |
| $^{216m}$Ac | 9.105±0.010 | ~0.5 | 97 ±0.5 | 9.14 | 0.390 | 17 |
| | 8.283±0.010 | ~0.5 | 3.0±0.5 | ... | ... | ... |
| $^{216}$Ac | 9.020±0.010 | ~0.5 | 98 ±0.5 | 9.14 | 0.390 | 17 |
| | 8.198±0.010 | ~0.5 | 2.0±0.5 | ... | ... | ... |
| $^{215}$Ra | 8.698±0.005 | 1.7±0.2 | 95.7±1.0 | 8.70 | 1.6 | 5,18 |
| | 8.168±0.008 | ~1.7 | 1.3±0.5 | ... | ... | ... |
| | 7.880±0.008 | ~1.7 | 3.0±0.5 | ... | ... | ... |
| $^{214m}$Fr | 8.549±0.008 | 3.6±0.5 | 51 ±2 | 8.546 | 3.42 | 19 |
| | 8.477±0.008 | 3.6±0.5 | 49 ±2 | 8.478 | 3.4 | 19 |
| $^{214}$Fr | 8.426±0.008 | 5.5±0.5 | 94.5±2.0 | 8.430 | 5.3 | 4 |
| | 8.353±0.008 | 5.5±0.5 | 5.5±0.5 | ... | 5.3 | ... |
| $^{213}$Rn | ... | ... | ... | 8.090 | 19 | 3,18 |
| $^{212m}$At | 7.899±0.008 | ... | 34 ±3 | 7.88 | 120 | 20 |
| | 7.837±0.008 | ... | 66 ±3 | 7.82 | 120 | 20 |
| $^{212}$At | 7.678±0.008 | ... | 80 ±3 | 7.66 | 305 | 20 |
| | 7.616±0.008 | ... | 20 ±3 | 7.60 | 305 | 20 |

$^{215}$Ac α group decayed with its previously reported[5] half-life of 170 msec and there was no 1.2 sec-component. From the data we can set an upper limit of 1.5% to the EC branching of $^{215}$Th.

### 3. *Thorium-214 and Thorium-213*

Regularities in α decay properties suggest that $^{214}$Th and $^{213}$Th should have closely similar energies between 7.65 and 7.73 MeV (see Fig. 9) and similar half-lives in the range 50 to 200 msec. The small peak at 7.68 MeV shown in Fig. 2 is assigned to these isotopes. The maximum of the excitation function shown in Figs. 3 and 4 falls in the proper energy range for a thorium isotope of lower mass than 215. The width of the excitation maximum is somewhat greater than expected for one isotope but on the other hand is not so broad as to indicate clearly that the 7.68-MeV α activity is a mixture of two isotopes. However, when the α-particle energy and the half-life were carefully measured at two widely spaced points of the excitation function, different values were obtained. At a beam energy of 142 MeV an α energy of 7.680±0.010 MeV and a half-life of 125±25 msec were found and assigned to $^{214}$Th. At a beam energy of 157 MeV an α energy of 7.690±0.010 and a half-life of 150±25 msec were obtained and assigned to $^{213}$Th. These determinations are less certain than those for the higher mass thorium isotopes.

## C. Short-Lived Isotopes with 127 Neutrons

In Fig. 9 a pronounced break occurs in the variation of α energy with neutron number at the 126 neutron shell. The nuclides with 127 neutrons have much higher decay energies and, hence, shorter half-lives than do the nuclides with 126 or fewer neutrons. The half-lives of most of the 127 neutron nuclides are so short that in our previous studies with a longer helium transport time[1,5] we were able to observe them only if they were produced by the decay of a long-lived parent. In the present study, however, the transport time was sufficiently short so that we were able to collect and identify α groups from several of these nuclides including $^{217}$Th, $^{216}$Ac, $^{215}$Ra, and $^{214}$Fr. The nuclide $^{213}$Rn was not observed because it is gaseous and does not stick to the collector foil. A summary of our results on the 127-neutron nuclides is given in Table III. We include revised α energies of $^{212}$At and $^{212m}$At in the list although that isotope was not a subject of further study. The new information that we collected on these nuclides came as a result of our study of the thorium isotopes and is incomplete. A more definitive study would require additional work with a faster system and the investigation of other projectile target combinations.

### 1. *Thorium-217*

$^{217}$Th contains one neutron more than the filled 126-neutron shell. From the known half-lives of $^{216}$Ac, $^{215}$Ra, $^{214}$Fr, and $^{213}$Rn, which also have 127 neutrons each, the half-life of $^{217}$Th can be estimated to be between 50 and 200 μsec. From the systematic regularities in α-decay properties displayed in Fig. 9 the α energy of $^{217}$Th is predicted to lie between 9.20 and 9.35 MeV.

The speed characteristics of our chamber were not suitable for the study of such a short-lived activity and under the operating conditions used to measure most of our spectra we did not observe this activity. However, in half-life measurements that were run continuously during and between beam bursts (see the third mode of operation in Sec. II C), a very short-lived group was observed at 9.250±0.010 MeV. It was visible only in spectra taken during a few msec before and after the end of each beam burst. The spectrum shown in Fig. 5 was obtained by combining two such spectra. We obtained an upper limit of 0.3 msec for the half-life.

Similar measurements during and just after the beam burst were made at other beam energies and the results were used to determine a rough excitation function for the 9.250-MeV group. This curve is drawn with a

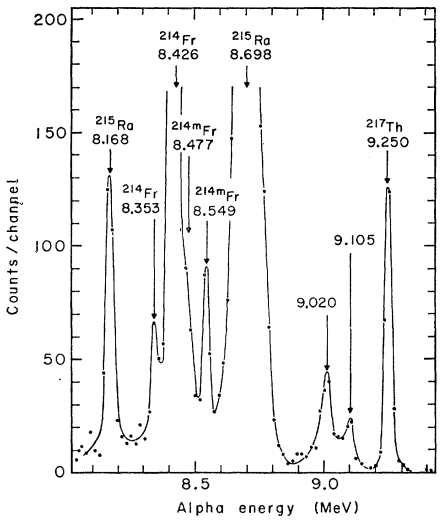


FIG. 5. $\alpha$ spectrum showing the 9.250-MeV group of $^{217}$Th and a few other groups. The spectrum was obtained by adding together two runs made at 96- and 106-MeV beam energies, respectively. The counting was performed during a period of 1.8 msec after the end of each beam burst.

broken line in Fig. 3 to indicate that it comes from a separate set of measurements. The curve has a shape typical for a compound nucleus reaction. The yield maximum at 102-MeV beam energy corresponds to an excitation energy of 57 MeV for the compound nucleus $^{222}$Th (Table I). This is a proper amount for the evaporation of five neutrons in the de-excitation process, indicating strongly that the 9.250-MeV activity belongs to $^{217}$Th.

### 2. *Actinium-216*

Rotter *et al.*[17] reported a half-life of 0.39±0.03 msec and an $\alpha$ energy of 9.14±0.03 MeV for $^{216}$Ac prepared by the reaction of $^{12}$C ions with $^{209}$Bi in the Dubna cyclotron. In our $\alpha$ spectra from products of the $^{206}$Pb+$^{16}$O reaction we observed two weak peaks of approximately equal intensity at 9.020 and 9.105 MeV. We verified that this was the same activity observed by Rotter *et al.* by identifying the same two groups in samples prepared by their method; when a $^{209}$Bi target was bombarded with 88-MeV $^{12}$C ions the 9.020- and 9.105-MeV peaks were observed in good yield. On such samples the half-life was measured by the technique discussed in Sec. II C with spectra recorded for 1-msec intervals during and after the beam burst. The result, shown in Fig. 6, indicates an apparent half-life of 0.56 msec. The ratio of the 9.020- and 9.105-MeV peaks remained 1:1 throughout the measurement. This half-life is an upper limit because of the influence of the transport time and the true value is about 0.5 msec. We do not completely understand why our method gives a value so much longer than the 0.39-msec value reported by

[17] Kh. Rotter, A. G. Demin, L. P. Pashchenko, and Kh. F. Brinkmann, Yad. Fiz. 4, 246 (1966) [English transl.: Soviet J. Nucl. Phys. 4, 178 (1967)].

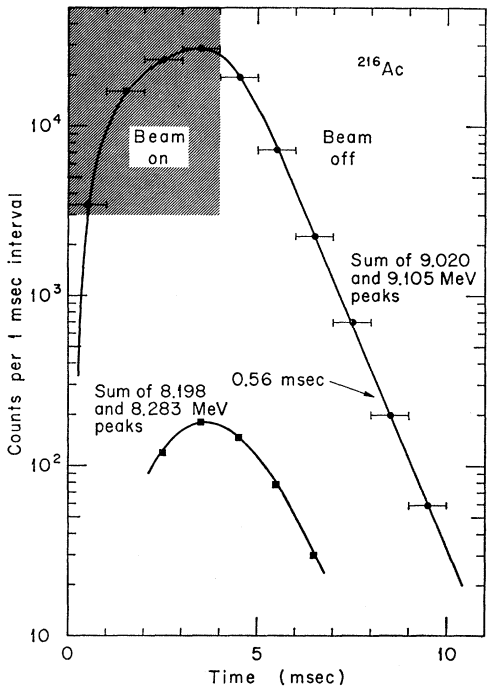


FIG. 6. Measurement of half-life of $^{216}$Ac prepared in the reaction of $^{209}$Bi with 88-MeV $^{12}$C ions. Experimental points show activity registered in counter during 1-msec periods starting at the beginning of the 4-msec beam burst and continuing 6 msec past the end of the beam burst. Upper curve shows sum of 9.020- and 9.105-MeV peaks. Lower curve shows sum of 8.198- and 8.283-MeV peaks.

Rotter *et al.*,[17] but as their value was determined in a more direct way it should be the more correct.

In the course of these half-life measurements we observed that two small peaks at 8.198 and 8.283 MeV also had the same growth and decay characteristics (see Fig. 6).

For confirmation of the results on $^{216}$Ac we prepared additional samples by the bombardment of $^{205}$Tl with $^{16}$O. Based on our previous excitation functions[5] for $^{214}$Ac and $^{215}$Ac produced by $^{205}$Tl($^{16}$O,$xn$) reactions, we chose a bombardment energy of 100 MeV for maximum production of $^{216}$Ac. Under these conditions the 9.020- and 9.105-MeV peaks were observed in good yield and in equal abundance (±2%) as shown in Fig. 7. In addition the small peaks at 8.198 and 8.283 MeV were reproduced (see, also, Fig. 7). A half-life measurement gave results for the combined 9.020- and 9.105-MeV peaks and the combined 8.198- and 8.283-MeV peaks identical to those shown in Fig. 6.

The energy separation between the 8.198- and 8.283-MeV peaks is 85 keV, which is the same as the energy separation of the prominent 9.020- and 9.105-MeV peaks. Isomerism is to be expected in $^{216}$Ac for the reasons discussed in Sec. IV C and it is our conclusion that the four peaks under discussion can be attributed to the decay of two isomeric forms of $^{216}$Ac separated in energy by 87 keV and having nearly

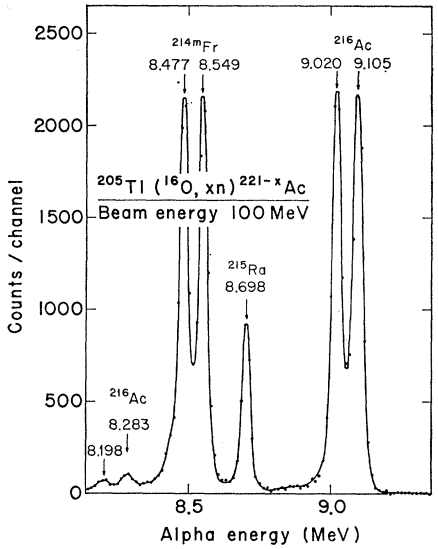


FIG. 7. $\alpha$ spectrum showing the four $\alpha$ groups of $^{216}$Ac prepared in the reaction of $^{205}$Tl with 100-MeV oxygen ions.

identical half-lives. The radiations assigned to the two forms are as follows: $^{216m}$Ac [8.283 MeV (3±0.5)%, 9.105 MeV (97±0.5)%] and $^{216}$Ac [8.198 MeV (2±0.5)%, 9.020 MeV (98±0.5)%]. All of our observations of the behavior of these four peaks in the $^{209}$Bi+$^{12}$C and $^{205}$Tl+$^{16}$O reactions are consistent with these assignments. Nonetheless, this interpretation is speculative.

In the case of the $^{206}$Pb+$^{16}$O reaction we encountered some interference in our study of the 9.020- and 9.105-MeV peaks owing to the presence of an additional peak at 9.01±0.02 MeV with a half-life of 25±2 msec. For example, at an $^{16}$O ion energy of 96 MeV, the 9.01-MeV peak with a 25-msec half-life was fourfold greater than the 9.105-MeV peak, the latter having a half-life of 0.5 msec. Preliminary work, not discussed in this report, indicates that this 9.01-MeV $\alpha$ activity is $^{216}$Fr kept alive by a 25-msec $^{220}$Ac parent. The possibility that this activity could be an isomer of $^{216}$Ac formed by the electron-capture decay of 28-msec $^{216}$Th was eliminated by noting that the yield variations of the 9.01-MeV activity and of $^{216}$Th with $^{16}$O ion energy were markedly different.

### 3. Radium-215

The earliest information on $^{215}$Ra came from an unpublished study of Griffioen and Macfarlane,[18] who reported a half-life of 1.6 msec and an $\alpha$ energy of 8.7 MeV. Rotter *et al.*[17] reported an energy value of 8.73 MeV. In our previous study of actinium isotopes[5] we observed a peak at 8.70±0.02 MeV which we attributed to $^{215}$Ra formed by electron capture of $^{215}$Ac.

In the present study $^{215}$Ra was produced in abundance at all beam energies (see Fig. 2). Our revised value of

[18] R. D. Griffioen and R. D. Macfarlane (unpublished results).

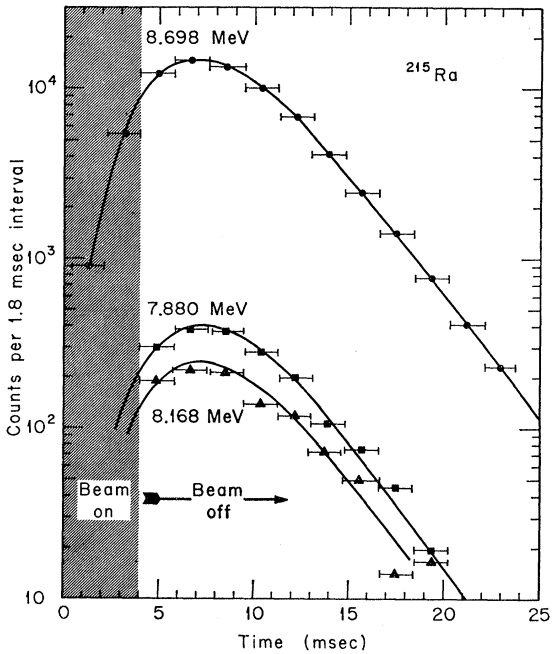


FIG. 8. Measurement of half-life of $^{215}$Ra prepared by the reaction of $^{206}$Pb with 96-MeV $^{16}$O ions. Experimental points show activity registered in detector during 1.8-msec periods starting at the beginning of a 4-msec beam burst and continuing in the period between beam bursts. The apparent half-life is 2.1 msec but correction for the effect of transport time reduces this to 1.7 msec.

the $\alpha$ energy is 8.698±0.005 MeV. The excitation function of this group is shown in Fig. 3.

We have evidence for two groups in lesser intensity. At a beam energy of 95 MeV where $^{215}$Ra is produced in greatest intensity two weak groups were observed at 8.168±0.008 MeV and 7.880±0.008 MeV (Fig. 2). Insofar as the excitation functions for these peaks could be followed (Fig. 3), they were parallel to that of the intense 8.698-MeV group. Interference from the 7.921-MeV group of $^{216}$Th made it impossible to observe the 7.880-MeV group at beam energies above 100 MeV. Measurement of the half-lives of the three $^{215}$Ra groups is illustrated in Fig. 8. Within the statistical scatter of the data points the decay curves of the 8.168- and 7.880-MeV groups are similar to that of the 8.698-MeV group. Additional evidence for the assignments came from bombardments of separated $^{206}$Pb and $^{208}$Pb with $^{20}$Ne. The 8.168- and 7.880-MeV peaks were observed in those spectra only at beam energies where the yield of the 8.698-MeV group was at maximum.

The relative intensities of the three $^{215}$Ra groups are: 8.698 MeV 95.7±1.0%, 8.168 MeV 1.3±0.5%, and 7.880 MeV 3.0±0.5%. The half-life is 1.7±0.2 sec.

### 4. Francium-214

The first information about $^{214}$Fr came from an unpublished study by Griffioen and Macfarlane[18] according to which the half-life is 3.9 msec and the

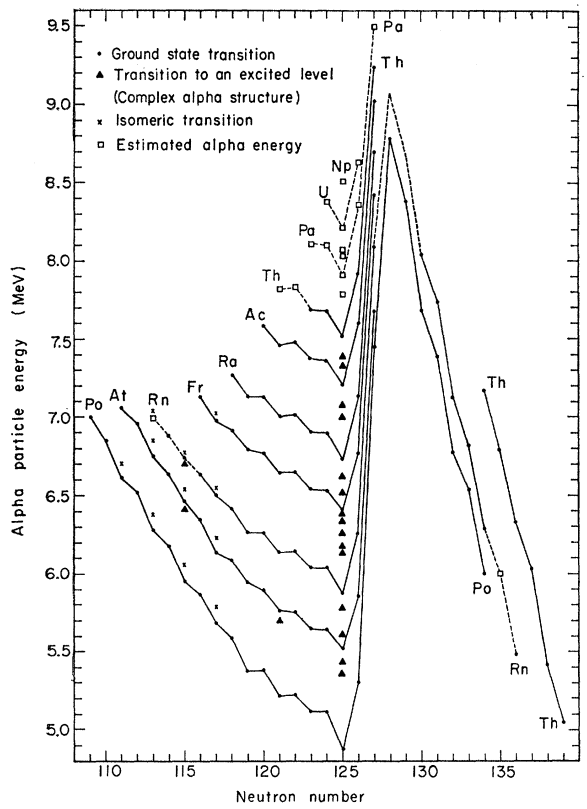


FIG. 9. $\alpha$ energy versus neutron number for isotopes of elements above lead in the vicinity of the 126-neutron shell.

$\alpha$ energy 8.55 MeV. Rotter *et al.*[17] reported an $\alpha$ energy of 8.53 MeV. In our previous study of radium isotopes[4] we found a weak $\alpha$ peak at 8.430±0.008 MeV with an excitation function and apparent half-life similar to 2.6-sec $^{214}$Ra and assigned it to $^{214}$Fr formed by electron capture decay of $^{214}$Ra. Somewhat later Torgerson, Gough, and Macfarlane[19] reported to us their observation of two $\alpha$ groups from $^{214}$Fr, one at 8.546 MeV, the other at 8.478 MeV, both with a half-life of about 3.4 msec, and called attention to the possibility of the occurrence of $^{214}$Fr isomers similar to the $^{212}$At isomers reported by Jones.[20]

In the present study we observed four $\alpha$ peaks which we assign to $^{214}$Fr with energy values 8.549, 8.477, 8.426, and 8.353 MeV, all with error limits of 0.008 MeV. The groups are shown in Figs. 2 and 5. A half-life of 3.6±0.5 msec was determined for the 8.549- and 8.477-MeV groups and 5.5±0.5 msec for the other two groups. The excitation functions of the 8.548- and 8.477-MeV groups (Fig. 4) differ considerably from those of the 8.426- and 8.353-MeV groups. This difference is analogous to the 15-MeV displacement of the excitation function for $^{149m}$Tb relative to that for $^{149}$Tb in reactions induced in $^{139}$La by $^{16}$O ions.[21] Shifts of this type can be caused by selective formation of the high-spin isomer from compound nuclei of high angular momentum.[21–23] Because of these differences in the half-lives and excitation functions, we assign the 8.426- and 8.353-MeV groups to the ground state of $^{214}$Fr and the other two groups to an isomer $^{214m}$Fr. Relative intensities of the $\alpha$ groups are given in Table III. The decay scheme of $^{214}$Fr is discussed further in Sec. IV C.[23a]

[19] D. Torgerson, R. Gough, and R. D. Macfarlane (McMaster University, Canada, private communication).
[20] W. B. Jones, Phys. Rev. **130**, 2042 (1963).

TABLE IV.[a] Estimated $\alpha$ energies of a few unknown neutron-deficient isotopes of thorium, protactinium, uranium, and neptunium. The predictions are based on the systematic regularities observed in the $\alpha$ decay of the light isotopes of the elements polonium through thorium.

| Isotope | $\alpha$ energy (MeV) | % |
|---|---|---|
| $^{211}$Th | 7.82±0.03 | |
| $^{212}$Th | 7.83±0.03 | |
| $^{214}$Pa | 8.11±0.03 | |
| $^{215}$Pa | 8.10±0.03 | |
| $^{216}$Pa | 7.91±0.03 | ~35 |
| | 7.79±0.03 | ~35 |
| | other groups | |
| $^{217}$Pa | 8.36±0.03 | |
| $^{218}$Pa | 9.50±0.10 | |
| $^{215}$U | 8.39±0.05 | |
| $^{216}$U | 8.38±0.05 | |
| $^{217}$U | 8.21±0.05 | ~40 |
| | 8.07±0.05 | ~50 |
| | 8.03±0.05 | ~10 |
| $^{218}$U | 8.63±0.05 | |
| $^{218}$Np | 8.51±0.07 | |
| | 8.41±0.07 | |
| | other groups | |

[a] We have observed a weak short-lived $\alpha$ group at 8.340±0.010 MeV in spectra obtained by bombardment of $^{203}$Tl and $^{206}$Pb with $^{20}$Ne ions, which on the basis of the evidence, can be assigned to $^{217}$Pa.

## IV. DISCUSSION

### A. α-Energy Systematics

It is of some interest to see how the new data on 23 $\alpha$ groups listed in Tables II and III fit in with the $\alpha$ data on neighboring nuclides. In Fig. 9 we present a revised plot of $\alpha$ energies versus neutron number. The systematic trends in this figure have been discussed in our previous reports.[4] By extrapolation of these curves it is possible to estimate unknown $\alpha$ energies for several nuclides with greater accuracy than is possible with existing mass formulas. In Table IV we list estimated $\alpha$ energies for a few unknown isotopes of thorium, protactinium, uranium, and neptunium. These estimated points are also shown in Fig. 9.

[21] R. D. Macfarlane, Phys. Rev. **126**, 274 (1962).
[22] G. N. Simonoff and J. M. Alexander, Phys. Rev. **133**, B104 (1964).
[23] J. M. Alexander and G. N. Simonoff, Phys. Rev. **130**, 2383 (1963).
[23a] *Footnote added in proof.* Additional information on the $\alpha$ radiations and the decay scheme of $^{214}$Fr has recently been published by D. F. Torgerson, R. A. Gough, and R. D. Macfarlane, Phys. Rev. **174**, 1494 (1968).

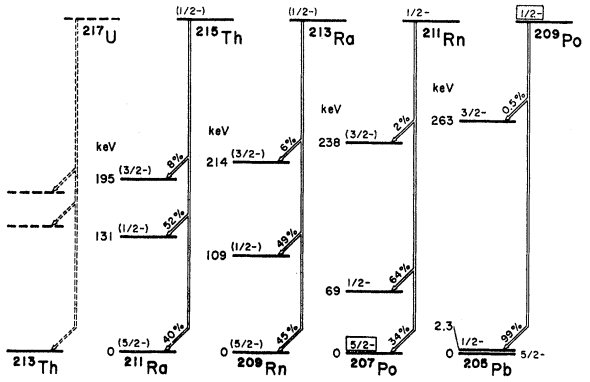


FIG. 10. $\alpha$ decay schemes of the 125-neutron isotopes of the even elements polonium, radon, radium, and thorium. The framed spin values have been measured directly, those shown without parentheses have been derived indirectly from extensive data, and those given in parentheses are our suggestions based principally on the apparent similarities between the schemes. The predicted decay scheme of $^{217}$U is indicated by broken lines.

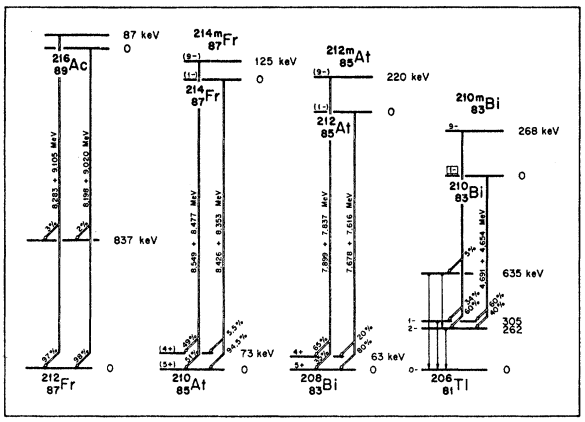


FIG. 11. $\alpha$ decay schemes of the 127-neutron isotopes of the odd elements bismuth, astatine, francium, and actinium. The framed spin value has been measured directly, those shown without parentheses have been derived indirectly, and those given in parentheses are our suggestions based on the shell-model predictions and the apparent similarities between the schemes.

### B. Complex $\alpha$ Decay of 125-Neutron Nuclei

Even-$Z$ nuclei with 125 neutrons have pronounced complex structure in their $\alpha$ spectra, which is of interest because it provides information on levels in the daughter nuclei. Figure 10 summarizes the data we wish to discuss. The data on $^{215}$Th come from the present study, those for $^{213}$Ra come from one of our previous papers,[4] and those for $^{211}$Rn and $^{209}$Po come from the references listed in *The Table of Isotopes*.[24] In the case of the daughter nuclei $^{205}$Pb and $^{207}$Po, many other excited levels are known but we show only the lowest-lying ones, which are the ones populated by $\alpha$ decay. The properties of the levels of $^{205}$Pb are well established and there seems little question that the $\frac{1}{2}$, $\frac{5}{2}$, and $\frac{3}{2}$ levels can be assigned to the $p_{1/2}$, $f_{5/2}$, and $p_{3/2}$ wave functions of the independent particle shell model. The $\frac{5}{2}$ and $\frac{1}{2}$ levels are also well established in $^{207}$Po and, in particular, the ground-state spin has been established to be $\frac{5}{2}$ by the work of Axensten and Olsmats.[25]

Figure 10 reveals a regular trend in the relationship of the three lowest levels and while the $\alpha$ spectra do not establish the spins of the levels in $^{209}$Rn and $^{211}$Ra it is tempting to make the assignments shown in parentheses and to regard the shifts in the level positions as a reflection of the operation of residual internucleon forces as the proton pairs are increased beyond the 82-proton shell. No one has treated this particular problem with any of the current theoretical models for the residual internucleon forces although the shift in these levels in going from $^{207}$Pb to $^{205}$Pb has been treated by several authors.[26,27]

Assuming that this identification of the levels shown in Fig. 10 is correct we can make the predictions of the levels of $^{213}$Th and the $\alpha$-decay pattern of $^{217}$U shown in Fig. 10 and in Table IV.

### C. Isomerism in Odd-Odd Nuclei with 127 Neutrons

As a result of the work of Jones[20] on $^{212}$At, of Torgerson, Gough, and Macfarlane[19] on $^{214}$Fr, of the present authors on $^{214}$Fr, and of the authors cited in *The Table of Isotopes*[24] on $^{210}$Bi, we now have proof of the systematic occurrence of isomerism in nuclides of odd elements above lead containing 127 neutrons. The cases are summarized in Fig. 11.

The isomerism can be explained by the high spins of the odd neutron and proton. The shell model predicts $g_{9/2}$ and $h_{9/2}$, respectively, so that close-lying levels of 0− and 9− are possible. The case of $^{210}$Bi is particularly interesting from the standpoint of theory[28] because it provides an opportunity to test the $np$ interaction for a single neutron and single proton of high spin beyond a double-closed-shell core. The residual interaction between these two particles gives rise to a multiplet of ten negative-parity levels with spins from zero to nine. The correct ordering of these levels seems to occur only if a short-range tensor force is added to a central force of the type successfully used to explain the $nn$ interaction in such nuclei as $^{206}$Pb. A particularly interesting feature in $^{210}$Bi is that the ground state is 1− rather than 0−. The 0− level occurs at 47 keV and then a wide spin gap occurs because the next state is 9− at 250 keV. Theoretical calculations on $^{212}$At, $^{214}$Fr, and $^{216}$Ac would be more complex because of the extra pairs of protons beyond the closed shell but the experimental results prove that a wide gap in spin is preserved in the ground-state multiplet, at least for the first two. The data also suggest strongly that 1−

[24] C. M. Lederer, J. M. Hollander, and I. Perlman, *Table of Isotopes* (John Wiley & Sons, Inc., New York, 1967), 6th ed.
[25] S. Axensten and C. M. Olsmats, Arkiv Fysik **19**, 461(1961).
[26] W. W. True, Nucl. Phys. **25**, 155 (1961).
[27] L. S. Kisslinger and R. A. Sorensen, Kgl. Danske Videnskab. Selskab, Mat.-Fys. Medd. **32**, No. 9 (1960).
[28] Y. E. Kim and J. O. Rasmussen, Nucl. Phys. **47**, 184 (1963).

rather than 0− is preserved as the ground state in $^{212}$At and $^{214}$Fr. This conclusion is reached because the pair of $\alpha$ groups from the isomer have the same energy separation as the pair from the ground state, indicating that the ground and first-excited states are being populated in both instances. But this could not be the case if the ground state of $^{212}$At or $^{214}$Fr were 0− because the selection rules of $\alpha$ decay would forbid a 0− to 4+ transition, and it is highly likely that the ground state and first-excited state of the daughter nuclei are 5+ and 4+, respectively, resulting from the coupling of $p_{1/2}$ neutron and $h_{9/2}$ proton.

In the case of $^{216}$Ac the systematic trends would suggest the occurrence of isomerism. As mentioned in Sec. III C *2*, we have observed four $\alpha$ groups which we tentatively attribute to isomeric decay in $^{216}$Ac. The proposed scheme is shown in Fig. 11.

## ACKNOWLEDGMENTS

We thank Dr. Albert Ghiorso for his interest in and support of this work. We are indebted to Richard Leres for the design of the electronic programmer used for the selection of mode of data collection and routing of data to the PDP-7 computer memory. We used the analog-to-digital converter unit and other interface hardware to the computer designed by Dr. Lloyd Robinson and employed his programs during data taking. Charles Corum contributed his usual excellent ideas to the mechanical design. Finally, we acknowledge the contributions of Professor R. D. Macfarlane to our program during a period of collaboration with one of us (KV) in the summer of 1967.

## APPENDIX A: RANGE CONSIDERATIONS

The recoil energies of the reaction products and their ranges play a role in the choice of chamber dimensions, helium pressure, and target thickness. Since we can be sure that the thorium isotopes are prepared by compound nucleus reactions involving full momentum transfer we can compute their kinetic energies and use the data obtained by others on recoil characteristics of reaction products from reactions induced by complex projectiles. If we assume isotropic emission of particles in the c.m. system of the compound nucleus, we can write

$$E_R = E_B A_R A_B / (A_B + A_T)^2, \quad \text{(A1)}$$

where kinetic energy and mass are represented by $E$ and $A$ and the subscripts $R$, $B$, and $T$ refer to the recoil nucleus, bombarding projectile, and target nucleus, respectively. According to this equation the recoil energies for the thorium isotopes of mass 213–217 produced in the $^{206}$Pb+$^{16}$O reactions are about 7% of the energy of the bombarding $^{16}$O ions. Hence from an $^{16}$O ion energy of 75 MeV, corresponding to the barrier energy, up to the full energy of 160 MeV the recoil energies of the thorium isotopes can vary from 5 to 11 MeV.

We can use the range data of Gilat and Alexander[29] on the range in helium of dysprosium recoil nuclei to estimate the range in helium of our products. For example, dysprosium ions of 5.8 MeV have a helium range of 453 $\mu$g/cm$^2$ equivalent to 2.6 cm at 1 atm pressure at room temperature, and 8-MeV dysprosium ions have a range of 560 $\mu$g/cm$^2$ equal to 3.3 cm. The higher atomic number thorium ions should have somewhat shorter ranges. A comparison of the ranges in aluminum absorbers of 5–11 MeV recoil ions of Dy, Sm, Tb, At, and Po indicates[30–33] that the range difference in light-element absorbers (helium in our case) for Dy and Th ions should be about 20–30%.

In most experiments our helium stopping path was 2.0 cm and the helium pressure was 1.9 atm, so that we had sufficient helium to stop the thorium recoils before they reached the back window, even without considering the slowing down in the target itself.

The stopping power of lead for heavy-element recoils is less than that of helium by a factor of 1.5 or 2. We have no data on recoil atoms as heavy as thorium but we can get some guidance from the measurements of Alexander and Winsberg[34] on the range of astatine recoil nuclei in gold. For example, 8.1-MeV ions have a range of 1.14 mg/cm$^2$. Our target thickness of 2.8 mg/cm$^2$ is greater than this, so that only those nuclei produced in the rear layer of the target emerged into the helium atmosphere.

Some of the other products such as the radium isotopes probably also have ranges corresponding to full momentum transfer. This is true whether these isotopes are made by the $\alpha$ decay of thorium parents or by $\alpha$ emission in the de-excitation of the compound nucleus. The work of Kaplan[35] is pertinent to this conclusion. For nuclei lighter than radium we may expect a variety of reactions not involving full momentum transfer to account for a considerable fraction of the yield. For example the recoil ranges of several polonium, astatine, and radon isotopes produced in the bombardment $^{197}$Au, $^{208}$Pb or $^{209}$Bi with $^{16}$O have been measured by Alexander and Winsberg[34] and by Croft *et al.*[36] In most cases the recoil ranges were far lower than expected on the basis of full momentum transfer, typically something of the order of a factor of 3 lower. We can expect in our case that the over-all yield for such reaction products is reduced because only those originating in a thin back layer of the target escape into the helium.

[29] J. Gilat and J. M. Alexander, Phys. Rev. **136**, B1298 (1964).
[30] L. Winsberg and J. M. Alexander, Phys. Rev. **121**, 518 (1961).
[31] J. M. Alexander and D. H. Sisson, Phys. Rev. **128**, 2288 (1962).
[32] M. Kaplan and R. D. Fink, Phys. Rev. **134**, B30 (1964).
[33] P. D. Croft and K. Street, Jr., Phys. Rev. **165**, 1375 (1968).
[34] J. M. Alexander and L. Winsberg, Phys. Rev. **121**, 529 (1961).
[35] M. Kaplan, Phys. Rev. **134**, B37 (1964).
[36] P. D. Croft, J. M. Alexander, and K. Street, Jr., Phys. Rev. **165**, 1380 (1968).

There is one small class of products for which an opposite trend occurs. In reactions of $^{209}$Bi with $^{16}$O near the Coulomb barrier some of the astatine and polonium products are known[36] to be ejected with energies substantially greater than those corresponding to full momentum transfer. Such a result can occur for reactions of low-impact parameter if the incoming projectile transfers a few nucleons to the target and the remainder of the projectile is then directed in the backward direction by Coulombic repulsion. It is possible that the $^{211}$Po observed in our spectra at the lower bombarding energies is formed by such a mechanism from $^{206}$Pb or from the 1.4% $^{208}$Pb contamination in the target.

Still another class of products is the fission products which, judging from previous measurements,[13,14] account for 75% of the total reaction. The fission products have energies comparable to those for the products of $^{235}$U fission induced by neutrons and hence their ranges are far greater than the ranges of the other reaction products. Most of them should penetrate the target and the helium gas to imbed themselves in the walls of the chamber.

## APPENDIX B: CHAMBER DESIGN NOTES

The range considerations covered in Appendix A play a role in the design of a chamber for work with short-lived nuclides. In principle the collection process can be accelerated by reducing the chamber volume or by increasing the helium flow rate. No particular problem arises for products of heavy-ion reactions with half-lives longer than a few tenths of a second because a chamber sufficiently small to permit an effective collection time of substantially less than one half-life is still large enough to accomodate a helium stopping path greater than the longest of the recoil ranges. However, when the half-lives are of the order of milliseconds or shorter, it is difficult to avoid a compromise between speed and range requirements in a choice of chamber dimensions. The key problem is the fact that the probability that the activity will stick to the collector foil drops quickly when the helium flow rate is increased beyond a certain point. Hence the use of a larger diameter capillary to increase speed or of a pressure higher than about 2 atm to decrease the range (and hence the chamber dimensions) is not permissible.

Nonetheless, the range considerations suggest some ideas to reduce the problem. For example, it may be possible to choose reaction conditions to make the desired product with a lower recoil energy. If it is made by a compound nucleus reaction, then, according to Eq. (1), the range can be reduced by using a low bombarding energy or a light projectile. For example, $^{214}$Fr can be made by the reactions $^{206}$Pb+$^{16}$O and $^{206}$Pb+$^{11}$B. In the first case the yield maximum occurs at a bombarding energy of 103 MeV (Fig. 4) and the recoil energy from Eq. (1) is 7.3 MeV. In the second case the peak of the excitation function would occur at about 55-MeV beam energy and the recoil energy would be about 2.7 MeV. If a spherical target chamber with a radius equal to one-half of the recoil range were used in each case and other conditions were kept unchanged, then the chamber volume in the $^{206}$Pb+$^{11}$B case would be about $\frac{1}{8}$ of that in the $^{206}$Pb+$^{16}$O case, and, accordingly, the smaller chamber would be eight times faster than the bigger one. In reactions induced by such particles as protons and deuterons, the recoil ranges are so short that a reaction chamber with a volume of the order of 0.1 cm$^3$ could be used to study nuclides with half-lives in the microsecond range.

In some cases the same product can be made in one reaction by a mechanism involving full momentum transfer or by another reaction in which only partial momentum transfer occurs and hence be produced with much less kinetic energy.

Another option is to use a thick target so that the recoiling nuclei are slowed down in the target itself and spend only a fraction of their range in the gas. The chamber volume can be decreased to take advantage of this but this, of course, involves some loss of yield because those products made in the back target layer are lost to the back wall of the chamber.

The present design of the target chamber has some advantages that may be valuable in other applications. The capillary can be made at least 20 cm long (probably much longer) without essential loss of speed or collection efficiency. This provides enough room for heavy shielding around the detector. Because of the small size of the target chamber most fission products are buried in the walls of the chamber which reduces the build-up of $\beta$ and $\gamma$ activity in the counting chamber. These properties were at considerable value in the present experiments, and they would be much more important in the application of the helium jet transport system to the collection of recoil nuclei for on-line study of $\gamma$ activity.